

## Diamond-Metal Interfaces and the Theory of Schottky Barriers

J. Ihm, Steven G. Louie,<sup>(a)</sup> and Marvin L. Cohen*Department of Physics, University of California, Berkeley, California 94720, and Materials and Molecular Research Division, Lawrence Berkeley Laboratory, Berkeley, California 94720*

(Received 27 December 1977)

A self-consistent pseudopotential calculation of the diamond-metal interface is used to examine interface states and empirical correlation for the dependence of the Schottky-barrier height and interface index,  $S$ , on ionicity. The properties of diamond are crucial because of its large gap and zero ionicity. Predictions based on experimental extrapolations give  $S \approx 0$ . Our calculations give  $S = 0.4$  and a barrier height of 2.2 eV; the latter is in good agreement with experiment.

The behavior of the diamond-metal interface is considered to be central to resolving important questions in the theory of Schottky barriers. The relevant properties of diamond which make this material unique are its large gap but zero ionicity parameter.<sup>1</sup> Theories and empirical correlations involving Schottky barriers have concentrated on the dependence of barrier properties on ionicity and band gap. Since for most materials large ionicity implies large gaps, the correlations with ionicity and band gap are hard to determine separately.

We present here results of a self-consistent nonlocal pseudopotential calculation for the metal-diamond interface. We find that the behavior of the diamond Schottky barrier can be quantitatively understood using a model based on metal-semiconductor hybrid states (metal-induced gap states<sup>2</sup>). These states are free-electron-like in the metal region and decay rapidly into the diamond part of the interface. These states determine the Fermi-level pinning and yield a barrier height of 2.2 eV which is in satisfactory agreement with the experimental value of 1.9 to 2.2 eV.<sup>3</sup>

For covalent (nonionic) Schottky barriers, like Si or Ge, the barrier height,  $\Phi_b$ , is found to be essentially independent of the metal contact used, i.e., Fermi-level pinning is independent of metal electronegativity. In contrast for ionic materials like  $\text{SiO}_2$ , the barrier height depends on the metal contact and increases almost linearly with metal electronegativity,  $\chi_m$ . The dependence of barrier height on metal electronegativity is measured by the interface index  $S \equiv \partial\Phi_b/\partial\chi_m$ . Throughout this Letter,  $S$  is in units of electron volts per electronegativity units. Kurtin, McGill, and Mead<sup>4</sup> have examined the dependence of  $S$  on semiconductor ionicity,  $\Delta\chi$ , and the properties of this curve (e.g., the sharp rise around  $\Delta\chi \sim 0.7$ ) (Fig. 1) have been the subject of many investigations.  $S \approx 0$  for Si and Ge and  $S \approx 1$  for  $\text{SiO}_2$  as described

above. If  $\Delta\chi$  is, in fact, the fundamental variable, then a diamond Schottky barrier should exhibit an  $S \approx 0$ .

The method we have employed here is similar to the one used in the calculation of metal-Si and metal-zincblende interfaces.<sup>2,5</sup> We consider a unit cell consisting of twelve layers of diamond with a (111) surface in intimate contact with a jellium slab having charge density corresponding to aluminum ( $r_s = 2.07$ ). The thickness of the metal slab is equivalent to twenty layers of diamond. For computational purpose, this slab geometry is repeated along the direction perpendicular to the interface so that we retain three-dimensional periodicity. This supercell is big enough to prevent significant interactions between neighboring interfaces. The jellium edge is assumed to lie one-half of the C-C bond length away from the diamond surface. For diamond, we used a nonlocal pseudopotential, obtained<sup>6</sup> by fitting to atomic spectra, which yields a good band structure for bulk diamond with a small number of plane waves ( $\sim 40$  plus another 50 through second-

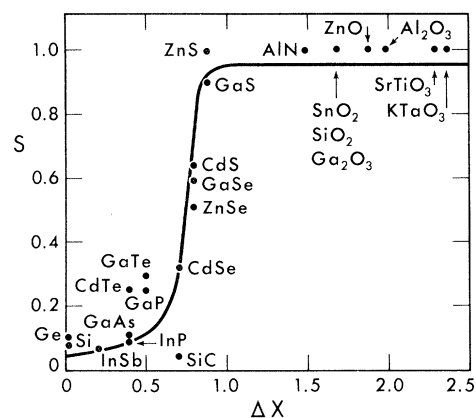


FIG. 1. The interface index,  $S$ , vs Pauling ionicity (from Ref. 4). For SiC the value of  $S$  has been adjusted to  $S \approx 0$  (Ref. 3).

order perturbation) in the basis set. The electronic wave function is expanded in a basis set consisting of 600 plane waves. Another  $\sim 800$  plane waves are included through a second-order perturbation scheme. This set of plane waves gives roughly the same degree of convergence as the bulk diamond or the diamond (111) surface calculations.<sup>6</sup> The final self-consistent charge density is obtained from six points in the irreducible two-dimensional Brillouin zone.

We will focus here only on gap states because it is these states that govern interface behavior. The charge density of the gap states is plotted in the (110) plane perpendicular to the interface in Fig. 2(a). The same charge-density profile,  $\bar{\rho}(z)$ , averaged parallel to the interface and plotted perpendicular to it, is shown in Fig. 2(b). These gap states are free-electron-like on the metal side and decay exponentially into the diamond region. True interface states localized at the interface do not exist for energies within the gap. The calculated barrier height,  $\Phi_b$ , defined here to be the difference between the Fermi level and the valence-band maximum of diamond (chosen for comparison with experiments done on *p*-type diamonds) is 2.2 eV. The experimental values range from 1.9 to 2.2 eV.<sup>3</sup> Image-force lowering is neglected in our calculation. The penetration of the metal-induced gap states into the diamond determines the behavior of  $\Phi_b$ . The extent of their penetration can be measured by a penetration

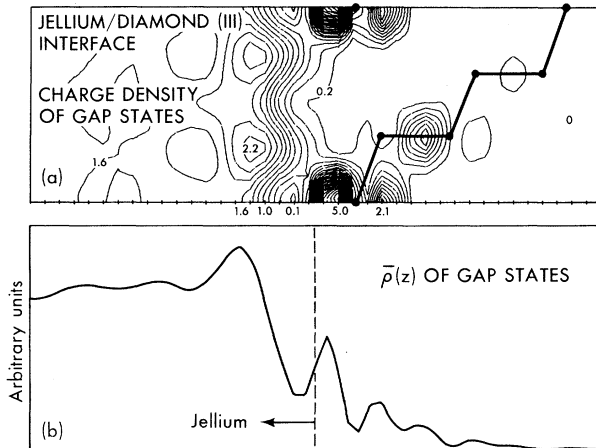


FIG. 2. (a) Charge-density contours for gap states with energies between 0 and 4 eV in a (110) plane. The numbers should be multiplied by 0.82 to get the number of electrons per unit cell of bulk diamond. (b) The same charge density averaged parallel to the interface and plotted along the direction perpendicular to the interface.

length  $\delta$  defined by

$$\bar{\rho}(\delta)/\bar{\rho}(0) = e^{-1}, \quad (1)$$

where the distance is measured from the interface to a point  $z$  inside the diamond. From Fig. 2(b),  $\delta$  is 1.37 Å. This value is roughly one-half of the corresponding decay length in the metal-Si ( $\sim 3.0$  Å)<sup>2</sup> or metal-Ge ( $\sim 2.7$  Å) interface.<sup>7</sup>

Another relevant quantity determining  $\Phi_b$  is the surface density of states,  $D_s(E)$ , defined by

$$D_s(E) \equiv A^{-1} \int_A \int_0^\infty N(E, \vec{r}) dz dA, \quad 0 < E < E_g, \quad (2)$$

where  $A$  is the interface area,  $E_g$  is the gap, and the integral over  $z$  is to be performed from the interface to a point deep into the bulk on the diamond side of the barrier.  $N(E, \vec{r})$  is a local density of states, defined by

$$N(E, \vec{r}) \equiv \sum_{n, \vec{k}} |\psi_{n, \vec{k}}(\vec{r})|^2 \delta[E - E_n(\vec{k})]. \quad (3)$$

Thus  $-eD_s(E)$  gives the density of surface charge per unit energy per unit area. The calculated  $D_s(E)$  shown in Fig. 3 is more or less uniform in the gap compared with the sharp peak of the dangling-bond surface states for the clean diamond

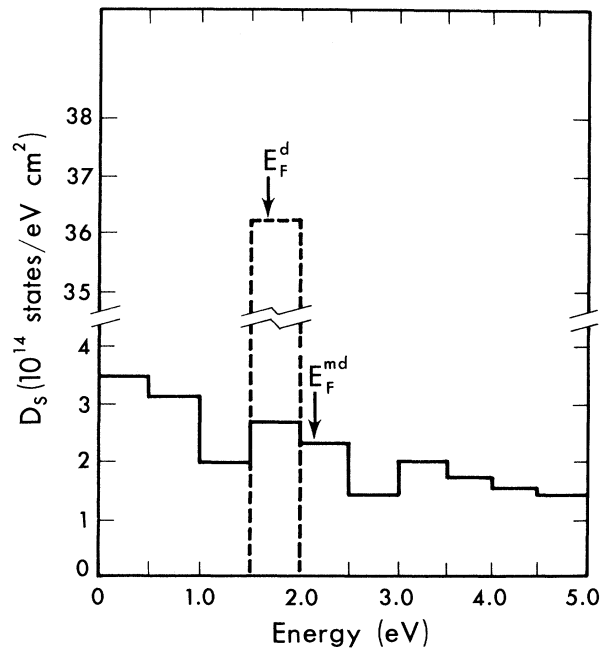


FIG. 3. Surface density of states,  $D_s$ , of the metal-diamond (111) interface in the gap. Also shown is the density of states of the clean diamond (111) surface states in the gap from Ref. 6. It is clear from the figure that the clean-diamond-surface-state peak is drastically reduced by the metal contact. The new metal-induced gap states give the uniform  $D_s$  shown above.

surface. Our calculation yields  $D_s(E_F) = 2.3 \times 10^{14}$  states/eV  $\cdot$  cm<sup>2</sup>. This is a dramatic change illustrating again that *it is not simply the dangling-bond states of the clean surface which determine the Schottky-barrier properties.*<sup>8</sup>

The  $S$  parameter can now be calculated using the following expression<sup>5</sup>:

$$S = 2.27 [1 + 4\pi e^2 D_s(E_F) (0.5 + \delta/\epsilon_s)]^{-1}, \quad (4)$$

where  $\epsilon_s$  is the dielectric constant for screening potential fluctuations within a distance of order  $\delta$ . We choose  $\epsilon_s \sim 2$ .<sup>9,10</sup> Although the present calculation of  $S$  does not include effects arising from the doping of diamond, it is known experimentally that  $\Phi_b$  is practically independent of doping density well above the typical doping density of  $n \sim 10^{17}$  cm<sup>-3</sup>. By substituting calculated values for  $\delta$  and  $D_s(E_F)$  into the Eq. (4), we obtain  $S = 0.38 \pm 0.1$ . The relatively large error bound is a consequence of the uncertainty in determining  $\delta$ ,  $D_s$ , and  $\epsilon_s$ . The only experimental value we are aware of supports a smaller value of  $S$  ( $S \approx 0.2$ ); however, the authors<sup>3</sup> point out that they do not consider this measurement to be conclusive.

Our result can be interpreted in terms of the energy gap,  $E_g$  and the lattice constant,  $a_c$ . Comparison with metal-Si and the metal-zincblende semiconductor interface calculations<sup>5</sup> indicates that the charge transfer per unit area to the semiconductor caused by the exponential tail of the metal-induced states in the thermal gap is proportional to the number of surface atoms of the semiconductor per unit area. In other words, each surface atom of the semiconductor "induces" (approximately) a fixed amount of charge transfer from the metallic wave functions on the other side. We estimate that 0.6–0.7 electronic states are available<sup>5,7</sup> on the semiconductor side in the thermal gap per surface atom of Si, GaAs, ZnSe, ZnS, Ge, and diamond. If this is the case, and if we assume that the surface density of states,  $D_s$ , is more or less uniform in the thermal gap, then a large-gap material has a small  $D_s$ . Neglecting lattice-constant effects, the  $D_s$  of diamond compared to Si would be reduced by a factor of the ratio of their gaps  $\sim \frac{1}{3}$ . However, since diamond has a smaller lattice constant than Si, it has a larger number of surface atoms per unit area; hence,  $D_s$  of diamond increases by a factor of the ratio of the squares of the lattice constants  $\sim 2.3$ . The net result gives an estimate for  $D_s$  of approximately one-half of the Si value ( $\sim 4.5 \times 10^{14}$  states/eV  $\cdot$  cm<sup>2</sup>). This is consistent with our computed value of  $2.3 \times 10^{14}$  states/eV  $\cdot$  cm<sup>2</sup>. Detailed

calculations showed that  $\delta$  is reduced roughly by the same factor. Another estimate of  $\delta$  using the one-dimensional WKB approximation [ $\hbar/2\delta = (n\bar{E}_g)^{1/2}$ , where  $\bar{E}_g$  is Phillips's gap<sup>1</sup>] gives results consistent with our detailed calculations.

We can use the above arguments to examine the case of cubic SiC. SiC is also an interesting test case because  $S$  for SiC should be greater than the corresponding value for Si or diamond if ionicity plays a central role. Experimentally the  $S$  parameter for SiC is uncertain; it is determined to be roughly as small as that of Si<sup>3</sup>. Using a gap of 2.3 eV and  $a_c = 4.35 \text{ \AA}$ ,<sup>11</sup> we estimate  $D_s$  for SiC to be given by

$$\frac{D_s(\text{SiC})}{D_s(\text{Si})} \approx \frac{1.1}{2.3} \left( \frac{5.43}{4.35} \right)^2 \approx 0.75. \quad (5)$$

Assuming the same reduction in  $\delta$ , we get  $S = 0.2$  which is half the corresponding value for diamond.

In conclusion, we obtain  $\Phi_b = 2.2$  eV and  $S \sim 0.4$  for the diamond Schottky barrier. If the above value for  $S$  is confirmed by experiment, this would support the conclusion that ionicity is not the fundamental parameter for the behavior of  $S$  (Fig. 1).

Recent suggestions to replace ionicity by chemical reactivity<sup>12</sup> or atomic term values<sup>13</sup> appear to predict  $S = 0$  for diamond. We suggest  $E_g a_c^2$  as a scaling parameter for  $S$ . Although this parameter does not give a sharp transition in the  $S$  curve (see  $\Delta\chi = 0.7$  in Fig. 1), Schlüter<sup>14</sup> has reexamined all available data and has also questioned the conventional interpretation and the sharp transition.

Two effects are not included in our calculation: chemical bonding between diamond and metal atoms, and reconstruction of the diamond surface at the interface.<sup>15</sup> Reconstruction greatly complicates the calculation and more detail is needed than is now available. Chemical bonding is not believed to be critical since we are doing linear Schottky-barrier theory and  $S$  is considered to be dependent on semiconductor properties only (to first order).

This work was supported by the Division of Basic Energy Sciences, U. S. Department of Energy and by the National Science Foundation Grant No. DMR76-20647.

(a) Present address: IBM Watson Research Center, P. O. Box 218, Yorktown Heights, N. Y. 10598.

<sup>1</sup>J. C. Phillips, *Bonds and Bands in Semiconductors*

(Academic, New York, 1973).

<sup>2</sup>S. G. Louie and M. L. Cohen, Phys. Rev. Lett. **35**, 866 (1975), and Phys. Rev. B **13**, 2461 (1976).

<sup>3</sup>C. A. Mead and T. C. McGill, Phys. Lett. **58A**, 249 (1976).

<sup>4</sup>S. Kurtin, T. C. McGill, and C. A. Mead, Phys. Rev. Lett. **22**, 1433 (1969).

<sup>5</sup>S. G. Louie, J. R. Chelikowsky, and M. L. Cohen, Phys. Rev. B **15**, 2154 (1977).

<sup>6</sup>J. Ihm, S. G. Louie, and M. L. Cohen, Phys. Rev. B **17**, 769 (1978).

<sup>7</sup>J. Ihm, S. G. Louie, and M. L. Cohen, to be published.

<sup>8</sup>J. Bardeen, Phys. Rev. **71**, 717 (1947).

<sup>9</sup>N. E. Brener, Phys. Rev. B **12**, 1487 (1975).

<sup>10</sup>P. E. Van Camp, V. E. Van Doren, and J. T. Devreese, J. Phys. C **9**, L79 (1976).

<sup>11</sup>R. C. Weast, *Handbook of Chemistry and Physics* (CRC Press, Cleveland, Ohio, 1977), 58th ed., p. E-101.

<sup>12</sup>L. J. Brillson, Phys. Rev. Lett. **40**, 280 (1978).

<sup>13</sup>E. J. Mele and J. D. Joannopoulos, to be published.

<sup>14</sup>M. Schlüter, private communication, and to be published.

<sup>15</sup>P. G. Lurie and J. M. Wilson, Surf. Sci. **65**, 453 (1977).

## Anomalous Propagation of Ultrasound in Metals by Open-Orbit Electrons

J. D. Gavenda and C. M. Casteel

*Department of Physics, The University of Texas at Austin, Austin, Texas 78712*

(Received 30 January 1978)

Open-orbit electrons are shown to generate an ultrasonic wave throughout a metal when the conditions for an open-orbit resonance are satisfied.

We have observed anomalous propagation of 30-MHz shear waves through copper and silver crystals by open-orbit electrons. At certain values of the applied magnetic field, acoustic energy from a wave packet of 1.0- $\mu$ sec duration spreads out over about 4.0  $\mu$ sec, reaching the receiver transducer long before the main body of the wave packet arrives. We first present the experimental data which suggested the effect, and then propose a simplified theoretical model which agrees with the principal features of the data.

Open-orbit electrons traveling parallel to the propagation vector  $\vec{q}$  of an ultrasonic wave absorb energy resonantly<sup>1</sup> when the period of the open orbit,  $D = \hbar K/eB$ , is some integral multiple  $n$  of the sound wavelength  $\lambda$ . Here  $\hbar K$  is the crystal momentum corresponding to the period of the open orbit in  $\vec{k}$  space,  $e$  is the electronic charge, and  $B$  the applied magnetic field. Hence, the resonance condition is  $B_n = \hbar K/ne\lambda$ .

While studying these effects with shear waves in copper, we decided to mount the quartz transducers with their polarization vectors midway between the fast- and slow-mode directions so that we could measure both modes in the experiment. Figure 1(b) shows the attenuation for the fast mode. Open-orbit resonances (OOR) are seen at the expected field values, but superimposed on

the curve are small "beat" patterns at field values which correspond to OOR for the slow mode, as shown in Fig. 1(a). In other words, it appears that some of the slow-mode signal arrives at the receiver transducer simultaneously with the fast-mode signal, but only when  $B$  corresponds to a slow-mode OOR. Furthermore, the phase of the anomalous slow-mode signal must be linearly proportional to  $B/B_n$  in order to produce the observed beats.

Direct observation of the signal from the receiver transducer shows that the slow-mode wave packet does indeed spread out at OOR, as shown in Fig. 2. As  $B$  is swept through a resonance, not only does the amplitude of the packet diminish, but a signal at the sound frequency begins to spread out far in advance of the packet. In some cases the spreading effect is much more evident than the attenuation resonances. In our copper and silver specimens the  $n = 4$  and 5 OOR are not visible in the attenuation, but we can easily see the wave packet spread out at values of  $B_n$  which correspond to those resonances.

We use a highly simplified model calculation to show that open-orbit electrons pick up energy while traversing the packet, and then transfer it coherently back to the lattice outside the packet.

We first consider the situation where the wave